

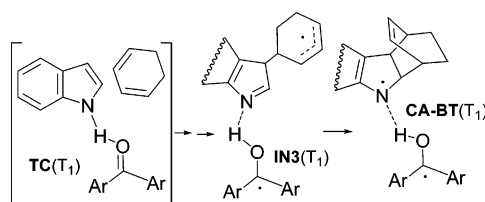
## Mechanism of Triplet Photosensitized Diels–Alder Reaction between Indoles and Cyclohexadienes: Theoretical Support for an Adiabatic Pathway

María González-Béjar,<sup>†</sup> Salah-Eddine Stiriba,<sup>†</sup> Luis R. Domingo,<sup>\*,†</sup> Julia Pérez-Prieto,<sup>\*,†</sup> and Miguel A. Miranda<sup>‡</sup>

*Instituto de Ciencia Molecular, Departamento de Química Orgánica, Universidad de Valencia, Polígono La Coma, 46980 Paterna, Valencia, Spain, and Departamento de Química/Instituto de Tecnología Química UPV-CSIC, Universidad Politécnica de Valencia, Camino de Vera s/n, 46071 Valencia, Spain*

*julia.perez@uv.es; domingo@utopia.uv.es*

*Received May 26, 2006*



Diels–Alder reactions between indoles (InHs) and 1,3-cyclohexadienes (CHDs) were achieved by using aromatic ketones as photosensitizers. For instance, irradiation of deaerated dichloromethane solutions containing benzoylthiophene (BT, 1 mM), indole (20 mM), and phellandrene (40 mM), in the presence of an acylating agent, led to the N-acetylated Diels–Alder cycloadduct in 46% yield (*endo:exo* ratio of 1.8:1). Energy transfer from the BT triplet to the CHD gave rise to diene dimers as byproducts. Several combinations of CHDs, InHs, and aromatic ketones were tested; the Diels–Alder reaction was found to be a general process, except when the indole nucleus was substituted at position 2 or 7 and when aromatization of the CHD was favored. Theoretical calculations support a stepwise mechanism involving a triplet ternary complex  $TC(T_1)$ , arising from a nearly barrierless reaction between CHD and the  $^3(BT\cdots HIn)^*$  exciplex. All subsequent steps proceed downhill in the triplet excited state, leading to a triplet cycloadduct-sensitizer  $CA-BT(T_1)$  radical pair. Attempts to detect this species, which is basically an aminyl/BT ketyl radical pair, were performed by laser excitation of a solution containing BT, phellandrene, and indole. The observed transient absorption spectra could be compatible with the added spectra of the expected components of the radical pair.

### Introduction

The Diels–Alder reaction is a well-established synthetic method that allows creation of two new carbon–carbon bonds, leading to the formation of six-membered rings. However, this reaction is generally inefficient when both diene (D) and dienophile (A) components are electron-rich compounds.<sup>1,2</sup>

Several strategies have been devised to overcome this limitation.<sup>3–6</sup> One of them makes use of singlet photosensitizers ( $^1S^*$ ), such as cyanoarenes,<sup>5</sup> and is postulated to operate through  $^1(S-A-D)^*$  ternary excited-state complexes (singlet triplexes).

<sup>†</sup> Universidad de Valencia.

<sup>‡</sup> Universidad Politécnica de Valencia.

(1) (a) An interesting exception is the Diels–Alder reaction between  $C_{60}$  and Danishefsky's dienes: Mikami, K.; Matsumoto, S.; Okubo, Y.; Fujitsuka, M.; Ito, O.; Suenobu, T.; Fukuzumi, S. *J. Am. Chem. Soc.* **2000**, *122*, 2236. (b) strained dienophiles can also lead to [4 + 2] adducts: Collins, S. K.; Yap, G. P. A.; Fallis, A. G. *Org. Lett.* **2002**, *4*, 11.

(2) Some thermal Diels–Alder reactions between electron-rich components are metal-catalyzed processes: Hilt, G.; Smolko, K. I. *Synthesis* **2002**, 686.

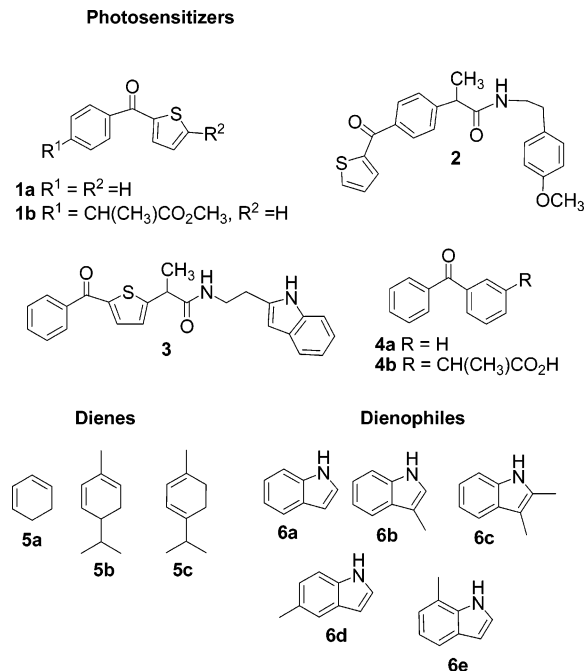
(3) (a) Mattay, J.; Trampe, G.; Runsink, J. *Chem. Ber.* **1988**, *121*, 1991. (b) Mattay, J.; Vondenhof, M.; Denig, R. *Chem. Ber.* **1989**, *122*, 951.

(4) (a) Pabon, R. A.; Bellvile, D. J.; Bauld, N. L. *J. Am. Chem. Soc.* **1983**, *105*, 5158. (b) Schmittel, M.; von Seggern, H. *J. Am. Chem. Soc.* **1993**, *115*, 2165. (c) Bauld, N. L.; Yang, J.; Gao, D. *J. Chem. Soc., Perkin Trans. 2* **2000**, 207.

(5) (a) Calhoun, G. C.; Schuster, G. B. *Tetrahedron Lett.* **1986**, *27*, 911. (b) Akbulut, N.; Hartsough, D.; Kim, J. I.; Schuster, G. B. *J. Org. Chem.* **1989**, *54*, 2549. (c) Kim, J. I.; Schuster, G. B. *J. Am. Chem. Soc.* **1992**, *114*, 9309.

(6) (a) Gieseler, A.; Steckhan, E.; Wiest, O.; Knoch, F. *J. Org. Chem.* **1991**, *56*, 1405. (b) Wiest, O.; Steckhan, E. *Tetrahedron Lett.* **1993**, *34*, 6391.

## CHART 1. Structures of the Photosensitizers, Dienes, and Dienophiles



Alternatively, electron-transfer photosensitizers such as triarylpyrylium salts have been employed, in which case the reaction proceeds via radical cations. In general, attempts to carry out Diels–Alder reactions by means of triplet–triplet energy transfer photosensitization have been unsuccessful.<sup>3b,5b</sup> However, we have recently reported preliminary studies on the reaction of indoles (InHs) with 1,3-cyclohexadienes (CHDs) photocatalyzed by triplet benzoylthiophenes (BTs).<sup>7</sup>

Herein, we wish to report experimental and theoretical studies performed to gain an insight into the triplet photosensitized Diels–Alder reaction between indoles and cyclohexadienes. In addition to benzoylthiophenes BTs (**1a**, **1b**, **2**, and **3**), we have used benzophenones (**4a** and **4b**) as typical triplet photosensitizers (Chart 1). From the obtained results, it seems clear that <sup>3</sup>(ketone⋯InH⋯CHD)\* triplet ternary complexes make possible the formation of [4 + 2] InH–CHD cycloadducts via an adiabatic process occurring in the triplet excited-state energy surface. Formation of an imine intermediate followed by its intramolecular reaction with an allyl radical appears to be the key to this unprecedented triplet photosensitized Diels–Alder reaction.

## Results and Discussion

**Benzoylthiophenes 1a and 1b as Photosensitizers. Steady-State Studies.** Product studies were performed by irradiation (UVA lamp emitting at 400 nm ≥ λ ≥ 320 nm) of deaerated dichloromethane solutions of **1a** or **1b** (0.001 M), CHD (**5a**–**5c**, 0.04 M), and InH (**6a**–**6e**, 0.02 M) for 6–8 h. Previous reports on this reaction using triarylpyrylium salts as photosensitizers have stressed the need to protect the amino group of the nascent photoadduct.<sup>6</sup> Therefore, an acylation reagent (acetyl chloride/NaHCO<sub>3</sub>) was also added to the reaction mixture prior to irradiation.

## SCHEME 1. Diels–Alder Reaction Photocatalyzed by Triplet Photosensitizers

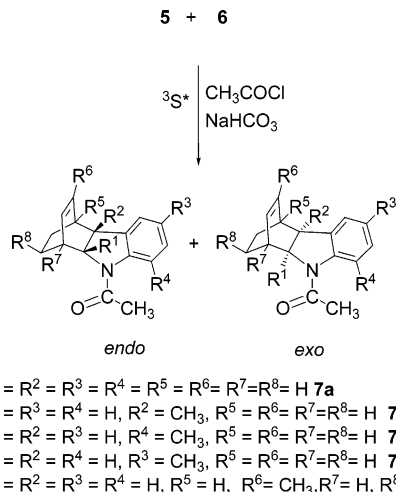


TABLE 1. Diels–Alder Reaction between Indoles and Cyclohexadienes upon Triplet Photosensitization in Dichloromethane

run	sensitizer	diene	indole	CHD-dimer yield (%) <sup>a</sup>	Diels–Alder yield (%) <sup>b</sup>	<i>endo:exo</i>
1	<b>1a</b>	<b>5a</b>	<b>6a</b>	38	<b>7a</b> <sup>c</sup> (15)	1.5:1.0
2	<b>1b</b>	<b>5a</b>	<b>6a</b>	27	<b>7a</b> (14)	1.4:1.0
3	<b>1a</b>	<b>5a</b>	-	99	-	-
4	<b>1a</b>	<b>5b</b>	<b>6a</b>	62	<b>7e</b> <sup>c</sup> (46)	1.8:1.0
5	<b>1b</b>	<b>5b</b>	<b>6a</b>	50	<b>7e</b> (37)	1.3:1.0
6	<b>1b</b>	<b>5b</b>	<b>6a</b> <sup>d</sup>	45	<b>7e</b> (24)	1.5:1.0
7	<b>1a</b>	<b>5a</b>	<b>6a</b> <sup>e</sup>	24	-	-
8	<b>1a</b>	<b>5b</b>	<b>6a</b> <sup>e</sup>	8	-	-
9	<b>1a</b>	<b>5b</b>	-	99	-	-
10	<b>1a</b>	<b>5a</b>	<b>6b</b>	10	<b>7b</b> (16)	1.5:1.0
11	<b>1a</b>	<b>5a</b>	<b>6d</b>	22	<b>7d</b> (19)	1.4:1.0
12	<b>2</b>	<b>5a</b>	<b>6a</b>	22	<b>7a</b> (12)	1.3:1.0
13	<b>3</b>	<b>5a</b> <sup>f</sup>	-	64	-	-
14	<b>3</b>	<b>5a</b> <sup>g</sup>	<b>6a</b>	32	<b>7a</b> (traces)	-
15	<b>4b</b>	<b>5a</b>	<b>6a</b>	41	<b>7a</b> (13)	1.5:1.0
16	<b>4a</b>	<b>5b</b>	<b>6a</b>	10	<b>8</b> (11)	1.5:1.0

<sup>a</sup> Relative to the initial amount of CHD. <sup>b</sup> Relative to the initial amount of indole. <sup>c</sup> Reference 6. <sup>d</sup> Performed at 0 °C. <sup>e</sup> In the absence of CH<sub>3</sub>COCl/NaHCO<sub>3</sub>. <sup>f</sup> [3] = 0.02 M, [5a] = 0.04 M. <sup>g</sup> [3] = 0.02 M, [5a] = 0.04 M, [6a] = 0.02 M.

Indeed, the acylated Diels–Alder products **7a** were obtained in ca. 15% yield, with an *endo:exo* ratio lower than 1.5:1 (Scheme 1 and runs 1 and 2 in Table 1). Energy transfer from the BT π,π\* triplet excited state (E<sub>T</sub> = 63 kcal/mol)<sup>8</sup> to **5a** (E<sub>T</sub> = 52 kcal/mol)<sup>9</sup> led to CHD dimers as byproducts, with an isomer distribution typical of a triplet-sensitized dimerization (*anti*-[2 + 2], *syn*-[2 + 2] and *exo*-[4 + 2] in a 3:1:1 ratio). By comparison, irradiation of BT with CHD, in the absence of indole, led to complete diene dimerization (run 3, Table 1 and Scheme 2, vi and 2vii).

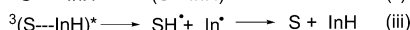
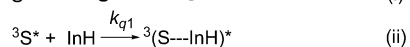
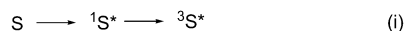
Cyclohexadienes other than the parent CHD were tested in the cross-cycloaddition with InH. The 2,5-disubstituted derivative **5b** led to a much higher yield of Diels–Alder products **7e** (compare runs 1 and 4 or runs 2 and 5 in Table 1). Interestingly, a lower reaction temperature (0 °C) was associated with a decrease in the reactivity mainly affecting the yield of Diels–Alder product (see run 6 in Table 1).

(7) Pérez-Prieto, J.; Stiriba, S.-E.; González-Béjar, M.; Domingo, L. R.; Miranda, M. A. *Org. Lett.* **2004**, *6*, 3905.

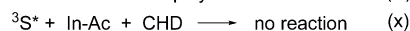
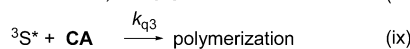
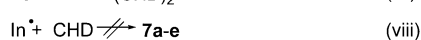
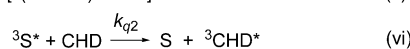
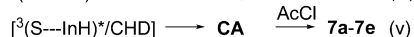
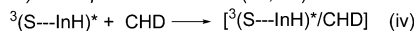
(8) Arnold, D. R.; Birtwell, R. J. *J. Am. Chem. Soc.* **1973**, *95*, 4599.  
 (9) Chung, W. S.; Turro, N. J. *J. Org. Chem.* **1989**, *54*, 4881.

## SCHEME 2. Photosensitized Processes

a) In the absence of CHD



b) In the presence of CHD (5a, 5b)

(S = 1a, 1b, 2, 4a, 4b)  
(InH = 6a-6e)

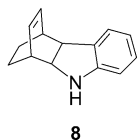
$$k_1 = k_{q1}[\mathbf{6a}] = 0.02 \times 2.0 \times 10^9 \text{ s}^{-1} = 4.0 \times 10^7 \text{ s}^{-1}$$

$$\text{for } \mathbf{5a}: k_2 = k_{q2}[\mathbf{5a}] = 4.7 \times 10^9 \text{ s}^{-1} \times 0.04 = 18.8 \times 10^7 \text{ s}^{-1}$$

$$\text{for } \mathbf{5b}: k_2 = k_{q2}[\mathbf{5b}] = 0.04 \times 3.9 \times 10^9 \text{ s}^{-1} \times 0.04 = 15.6 \times 10^7 \text{ s}^{-1}$$

$$k_{q3} = 2.0 \times 10^9 \text{ M}^{-1} \text{ s}^{-1}$$

as example of CA:



The regioselectivity found in the cycloaddition between **5b** and **6a** was similar to that found for the pyrylium salt-photosensitized electron-transfer process.<sup>6</sup> However, in the latter case the efficiency of cross-cycloaddition with diene **5a** was very similar to that found with **5b**.

As in the case of **5a**, energy transfer from the BT triplet to **5b** in the absence of indole led to diene dimers (run 9, Table 1) with a distribution typical of a triplet-sensitized dimerization.<sup>10</sup>

No Diels–Alder adducts were obtained with a 1,4-disubstituted cyclohexadiene such as  $\alpha$ -terpinene (**5c**), which underwent aromatization as the only observed reaction. Steric hindrance at the attacked CHD positions, together with the much lower oxidation potential (1.2–1.3 V for **5c** vs 1.8 for **5a**),<sup>11</sup> make aromatization via the diene cation radical<sup>12</sup> a competitive process ( $\Delta G = 5 \text{ kcal mol}^{-1}$ ). This could also be the reason for the reduced yield of Diels–Alder cycloadduct obtained in the pyrylium salt-photosensitized reaction between **5c** and **6a**.

Substitution at the indole ring (as in **6b–6e**) showed a clear influence on the photochemically induced cross-cycloaddition. Thus, whereas **6b** or **6d** gave rise to the corresponding photoadducts **7b** or **7d** (runs 10 and 11 in Table 1), Diels–Alder products were not detected when using **6c** and **6e** as dienophiles. By comparison, 2-methylindole does not lead to photoadducts in the pyrylium salt-photosensitized processes, and methyl 3-indolyl acetate reacts only sluggishly.<sup>6</sup>

Control experiments showed that *N*-acetylindole was not formed under the reaction conditions, since irradiation of a

mixture of *N*-acetylindole and CHD in the presence of **1a** did not give rise to adduct **7a** (Scheme 2, x). Besides, attempts to accomplish the BT-photosensitized Diels–Alder reaction in the absence of the acylation reagent were unsuccessful (see runs 7 and 8 in Table 1). These data agree well with acylation taking place after adduct formation (dark reaction, see Scheme 2, v). Also, they suggest that the unacylated photoadduct could be unstable under the irradiation conditions. As a matter of fact, when photoadduct **8** was irradiated in the presence of **1a**, analysis of the photolyzate by GC–MS and NMR showed the complete disappearance of **8** after 6 h of irradiation, although no well-defined, low molecular weight product was detected (Scheme 2, ix). Accordingly, laser flash photolysis (LFP) experiments showed that **8** acts as BT triplet quencher (vide infra).

**Time-Resolved Studies.** Laser excitation (Nd:YAG, 10 ns laser pulse, 355 nm) of deaerated dichloromethane solutions containing **1a** (1.6 mM) and the dienophile showed in all cases quenching ( $k_q = 2.0 \times 10^9 \text{ M}^{-1} \text{ s}^{-1}$ ) of the ketone  $\pi, \pi^*$  triplet ( $\lambda_{\text{max}}$  at 350 and 600 nm),<sup>13</sup> with concomitant formation of the corresponding BT ketyl ( $\lambda_{\text{max}}$  at 350 and 580 nm)<sup>14</sup> and indolyl ( $\lambda_{\text{max}}$  at 320 and 510 nm)<sup>15</sup> radicals (Scheme 2, iii); the quantum yield was close to 1. Figure 1 shows representative spectra for **1a**, **1a/6d**, and **1a/6e**. In the absence of CHD, regeneration of the starting materials is the main reaction in all cases (Scheme 2, iii); however, Diels–Alder photoadducts are not obtained upon irradiation of **1a/5a/6e** mixture, indicating that indolyl radicals do not play a key role in the cycloaddition process (Scheme 2, viii).

On the other hand, kinetic evaluation of **1a** triplet quenching by diene **5a** and Diels–Alder adduct **8** was performed (Figure 2, A and B). The slope of the linear plots provided the second-order rate constant ( $k_2$ ) for the quenching process by **5a** ( $4.7 \times 10^9 \text{ M}^{-1} \text{ s}^{-1}$ ) and **8** ( $2.3 \times 10^9 \text{ M}^{-1} \text{ s}^{-1}$ ). These data agree with the existence of a competitive quenching of BT triplet by the nascent photoadduct **8** (Scheme 2, ix), which decreases CHD dimerization when the reactions were carried out in the absence, compared to those in the presence, of the acylating agent (compare CHD dimerization in runs 1 and 7 in Table 1). Moreover, as mentioned above, quenching of the BT triplet by photoadduct **8** resulted in its polymerization (Scheme 2, ix).

**Comparative Studies with other Triplet Photosensitizers.** Previous solvent-dependence studies on the rate constants of **1a** triplet quenching by **6a**, together with density functional theoretical (DFT) calculations, agree with formation of a polarized hydrogen-bonded  $\text{BT}^{\delta-} \cdots \text{HIn}^{\delta+}$  exciplex (with a net charge of  $-0.28 \text{ e}$  at BT).<sup>14</sup> Also, the nonlinear increase of the quenching rate constant of BTs with increasing indole concentration has been taken as an evidence for the involvement of exciplex intermediates.<sup>16</sup> Hence, it appeared feasible that indoles act as dienophile components in Diels–Alder reactions, in processes that would actually involve triplet ternary complexes.

Therefore, we considered it of interest to study the behavior of aromatic ketones related to **1a**, having also high triplet quantum yields but different properties (triplet excited-state energies or lifetimes,  $n\pi^*$  character, etc.) as photosensitizers

(13) Becker, R. S.; Favaro, G.; Poggi, G.; Romani, A. *J. Phys. Chem.* **1995**, *99*, 1410.

(14) Pérez-Prieto, J.; Boscá, F.; Galian, R. E.; Lahoz, A.; Domingo, L. R.; Miranda, M. A. *J. Org. Chem.* **2003**, *68*, 5104.

(15) Jovanovic, S. V.; Steenken, S. *J. Phys. Chem.* **1992**, *96*, 6674.

(16) Pérez-Prieto, J.; Galian, R. E.; Morant-Miñana, M. C.; Miranda, M. A. *Chem. Commun.* **2005**, *68*, 3180.

(10) Baldwin, J. E.; Nelson, J. P. *J. Org. Chem.* **1966**, *31*, 336.

(11) (a) Schepp, N. P.; Johnston, L. J. *J. Am. Chem. Soc.* **1996**, *118*, 2872. (b) McManus, K. A.; Arnold, D. R. *Can. J. Chem.* **1994**, *72*, 2291.

(12) Climent, M. J.; Miranda, M. A.; Roth, H. D. *Eur. J. Org. Chem.* **2000**, 1563.

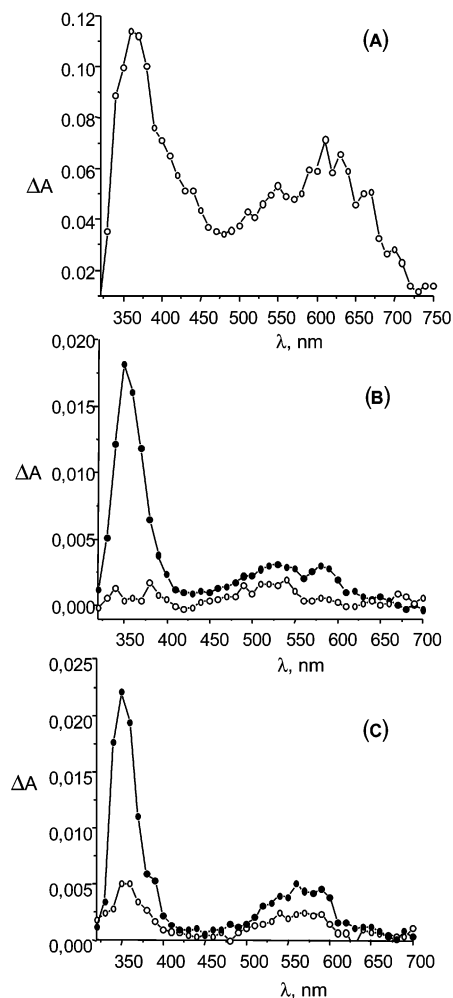


**FIGURE 1.** Transient absorption spectra at  $0.5 \mu\text{s}$  after the laser pulse (355 nm) of dichloromethane solutions containing BT (1.6 mM): (A) under nitrogen; (B) in the presence of **6d** (16.0 mM) under nitrogen (●) and oxygen (○) atmosphere; (C) in the presence of **6e** (16.0 mM) under nitrogen (●) and oxygen (○) atmosphere.

for the Diels–Alder reaction between indoles and dienes. Hence, 2-benzoylthiophene derivatives **2** and **3**, as well as benzenophenones **4a** and **4b** (Chart 1) were tested, and the results were compared with those obtained using **1a** and **1b**.

**Compound 2 as Photosensitizer.** The photophysical behavior of compound **2** in dichloromethane was similar to that of **1a**. Thus, time-resolved absorption spectra obtained after laser irradiation at 355 nm showed the formation of a triplet transient with absorption features similar to those of the 2-benzoylthiophene triplet (spectrum not shown). Intramolecular quenching by the anisole moiety was negligible.<sup>17</sup>

Product studies were performed by irradiation of deaerated dichloromethane solutions of **2** containing **5a**, **6a**, and the acylating agent, at room temperature. The results were similar to those obtained with **1a** (compare runs 1 and 12 in Table 1).

**Compound 3 as Photosensitizer.** The photophysical and photochemical behavior of several bichromophoric BT-InH compounds in methanol and acetonitrile solutions have already been reported.<sup>17,18</sup> At very short times after laser irradiation, only the transient absorption spectra of the corresponding ketyl-

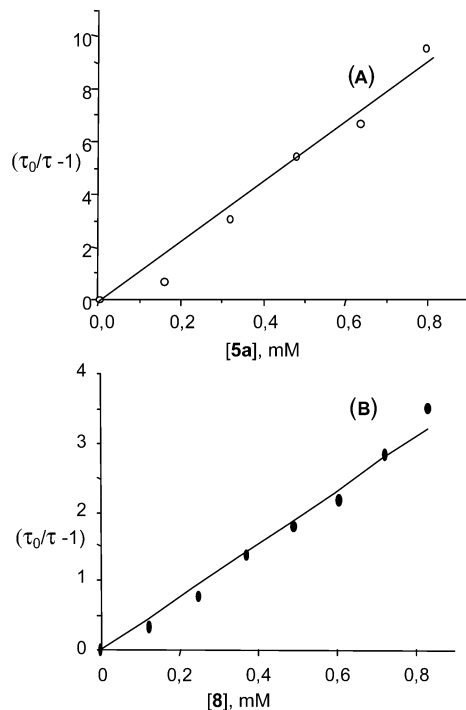


**FIGURE 2.** Stern–Volmer plots for triplet quenching of BT (1.6 mM) by (A) **5a** or (B) **8** in deaerated dichloromethane.

indolyl biradicals are observed with quantum yields close to one. This is the result of an intramolecular process, and any precursor of the biradicals must be formed within less than 50 ns. Theoretical DFT studies performed in a model BT-InH bichromophore have calculated a triplet energy of ca.  $56 \text{ kcal mol}^{-1}$  for the involved exciplex.<sup>18</sup> Therefore, it seemed worthy to study the ability of this exciplex to act as triplet photosensitizer, specially taking into account its presumable inability to form intermolecular hydrogen-bonded intermediates with added indole.

First, we checked whether CHD undergoes cycloaddition to the indolyl moiety of the photosensitizer. Thus, deaerated dichloromethane solutions of **3** (0.02 M) were irradiated (UVA lamp emitting at  $400 \text{ nm} \geq \lambda \geq 320 \text{ nm}$ ) for 6 h in the presence of 1,3-cyclohexadiene (CHD, **5a**, 0.04 M) and the acylating agent. Product studies did not allow to observe any cycloaddition of the diene to the indolyl group of **3**; however, CHD dimers were obtained in high yield (64%) and with an isomer distribution typical of triplet photosensitization (run 13, Table 1).

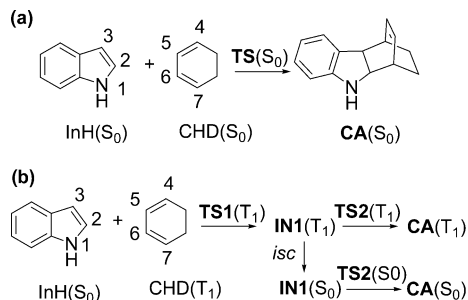
After realizing that **3** does not lead to Diels–Alder cycloadducts, it was tested as photosensitizer under the same conditions as those used with **1** and **2** (**3:5a:6a** ratio was 1:40:20). However, using catalytic amounts of **3**, the formation of photoadducts **7a** was only detected as traces by GC–MS. Besides, CHD dimers formation was reduced to 32% (see run 14 in Table 1).

**Benzophenones 4 as Photosensitizers.** Though the triplet of benzophenones **4** retains the capability to form hydrogen-bonded exciplexes with indole, its energy<sup>19a</sup> is  $6 \text{ kcal mol}^{-1}$

(18) Pérez-Prieto, J.; Stiriba, S.-E.; Bosca, F.; Lahoz, A.; Domingo, L. R.; Mourabit, F.; Monti, S.; Miranda, M. A. *J. Org. Chem.* **2004**, *69*, 8618.

(19) (a) Murov, S.; Carmichael, I.; Hug, G. L. In *Handbook of Photochemistry*, 2nd ed.; Marcel Dekker: New York, 1993. (b) Wilkinson, F.; Garner, A. *Photochem. Photobiol.* **1978**, *27*, 659.

(17) Pérez-Prieto, J.; Lahoz, A.; Bosca, F.; Martínez-Mañez, R.; Miranda, M. A. *J. Org. Chem.* **2004**, *69*, 374.

**SCHEME 3. Diels–Alder Cycloaddition at the Ground (a) and the Triplet Excited State (b).**

higher than that of  $^3\text{BT}$  and its electronic configuration is  $n\pi^*$  in nature. As in the case of BTs, laser irradiation of **4b** in the presence of indole evidenced the formation of ketyl (BPH) and indolyl radicals.<sup>19b</sup>

Product studies performed by irradiation of **4b** in the presence of **5a**, **6a** and the acylating agent showed that **7a** and CHD dimers are obtained in similar yields to the process photosensitized by **1a** and **1b** (compare run 15 with runs 1 and 2 in Table 1). However, when the substituted diene **5b** was used instead of the parent **5a** (see run 16 in Table 1), the results were clearly different and the reactivity was markedly lower. This could be related to the capability of  $n\pi^*$  aromatic ketones to achieve direct H-abstraction and to the fact that **5b** is a better H-donor than **5a**. Accordingly, comparison of the time-resolved spectra obtained after laser irradiation of **4a** at 355 nm in the absence and in the presence of **5b** revealed that quenching of the  $^3\text{BP}$  is partially associated with formation of the ketyl radical (BPH). By contrast, no new species were detected when similar experiments were performed with benzoylthiophene.

**Theoretical Studies.** The photoinduced Diels–Alder reaction between InH and CHD in the absence and in the presence of BT was studied theoretically using DFT methods at the UB3LYP/6-31G\* level. First, the reaction between InH and CHD in the ground ( $S_0$ ) and lowest triplet ( $T_1$ ) states was studied. Then, the photoinduced reaction between CHD and the  $^3(\text{BT}\cdots\text{HIn})^*$  triplet exciplex was considered.

**Diels–Alder Reaction between InH and CHD in the Ground ( $S_0$ ) and Excited Triplet ( $T_1$ ) States.** The reaction between InH and CHD in the  $S_0$  state takes place through a concerted bond formation process. Therefore, one transition structure, TS( $S_0$ ), and the corresponding cycloadduct CA( $S_0$ ) (see Scheme 3a) were located and analyzed. The geometry of TS( $S_0$ ) is given in Figure 3, and the energetic results are given in Table 2 and Figure 4.

The B3LYP/6-31G\* activation barrier for the Diels–Alder reaction between InH and CHD is 33.5 kcal mol<sup>-1</sup>. This large value, which is close to that computed for the dimerization of CHD at the  $S_0$  ground state (32.0 kcal mol<sup>-1</sup>)<sup>20</sup> prevents the cycloaddition process. Formation of the cycloadduct CA( $S_0$ ) is exothermic by -10.7 kcal mol<sup>-1</sup>. Note that while dimerization of CHD at the  $S_0$  ground state follows a stepwise mechanism with formation of a biradical intermediate,<sup>20</sup> the Diels–Alder reaction between InH and CHD at the  $S_0$  ground state is a concerted bond formation process.

In the triplet ( $T_1$ ) state the Diels–Alder reaction between InH and CHD appears to follow a stepwise mechanism. An exhaustive exploration of the potential energy surface (PES) at the

UB3LYP level allowed to find two TSs, TS1( $T_1$ ) and TS2( $T_1$ ), one biradical intermediate, IN1( $T_1$ ), and the cycloadduct CA( $T_1$ ) (see Scheme 3b). The geometries of the TSs are given in Figure 3, and the energetic results are given in Table 2 and in Figure 4.

The UB3LYP/6-31G\* activation barrier associated with formation of TS1( $T_1$ ) from CHD( $T_1$ ) plus InH( $S_0$ ) is 9.0 kcal mol<sup>-1</sup>. As a consequence, in the  $T_1$  triplet state a large acceleration of the Diels–Alder reaction is expected. The intermediate IN1( $T_1$ ) is located 8.9 kcal mol<sup>-1</sup> below the reactants. However, formation of the second C–C bond from this intermediate in the lowest  $T_1$  triplet surface via TS2( $T_1$ ) is uphill by 33.3 kcal mol<sup>-1</sup>. This would be the rate-limiting step for the triplet pathway, whose large barrier prevents the cyclization process. Formation of the cycloadduct CA( $T_1$ ) is endothermic by 14.7 kcal mol<sup>-1</sup>. However, the cycloaddition might take place along the ground state ( $S_0$ ) through a biradical intermediate IN1( $S_0$ ). Thus, we investigated the stepwise biradical path at the ground state ( $S_0$ ). Biradical IN1( $S_0$ ) and the associated TS, TS2( $S_0$ ), were located and characterized (see Scheme 3). However, all attempts to find TS1( $S_0$ ) were unsuccessful; all open shell calculations converge to TS( $S_0$ ).

Biradical IN1( $S_0$ ) is nearly isoenergetic with IN1( $T_1$ ); also, both intermediates present geometrically and electronically similar structures (vide infra). Formation of the second C–C bond to yield the Diels–Alder cycloadduct CA( $S_0$ ) takes place with a very low activation energy, 0.1 kcal mol<sup>-1</sup>. Triplet biradical IN1( $T_1$ ) is kinetically stable because an activation energy of almost 17.9 kcal mol<sup>-1</sup> is required to yield the reagents, InH( $S_0$ ) + CHD( $T_1$ ). Spin inversion at the allylic radical system of IN1( $T_1$ ) allows its conversion into IN1( $S_0$ ), which can give cycloadduct CA( $S_0$ ) in a barrierless process. These energetic results, which are similar to those found for the dimerization of CHD,<sup>20</sup> allow to explain the Diels–Alder reaction along a two-state mechanism involving intersystem crossing (ISC) from IN1( $T_1$ ) to IN1( $S_0$ ).

The UB3LYP/6-31G\* calculations give a barrier for the attack of CHD( $T_1$ ) to InH( $S_0$ ) via TS1( $T_1$ ) 4.6 kcal mol<sup>-1</sup> higher in energy than that found for the dimerization of CHD in the lowest  $T_1$  triplet state.<sup>20</sup> As a consequence, after excitation of CHD( $S_0$ ) to its triplet state, dimerization is faster than the Diels–Alder reaction between CHD and InH, in clear agreement with the experimental findings.

The geometries of TS( $S_0$ ), TS1( $T_1$ ), IN1( $S_0$ ), IN1( $T_1$ ), TS2( $S_0$ ), and TS2( $T_1$ ) are given in Figure 3. The lengths of the C3–C4 and C2–C7 bonds at TS( $S_0$ ) are 2.373 and 2.075 Å, respectively. These values indicate a concerted process, with bond formation at the C2 position of InH somewhat more advanced than at C3. In TS1( $T_1$ ) the C3–C4 bond length is 2.246 Å, while the distance between C2 and C7 is 4.120 Å. This large value indicates that the latter bond is not yet being formed at this step of the reaction.

In the biradical intermediates IN1( $T_1$ ) and IN1( $S_0$ ) the lengths of the C3–C4 bond are 1.575 and 1.580 Å, respectively, while the distances between C2 and C7 remain at 3.818 and 3.769 Å, respectively. The C5–C6 and C6–C7 bond lengths of these intermediates (ca. 1.39 Å) point to a C5–C6–C7 allyl arrangement in the cyclohexyl framework. In the TS for this ring-closure step, the C2–C7 bond length is 2.129 Å for TS2( $T_1$ ) and 3.181 Å for TS2( $S_0$ ).

(20) Domingo, L. R.; Pérez-Prieto, J. *ChemPhysChem* **2006**, *7*, 614.

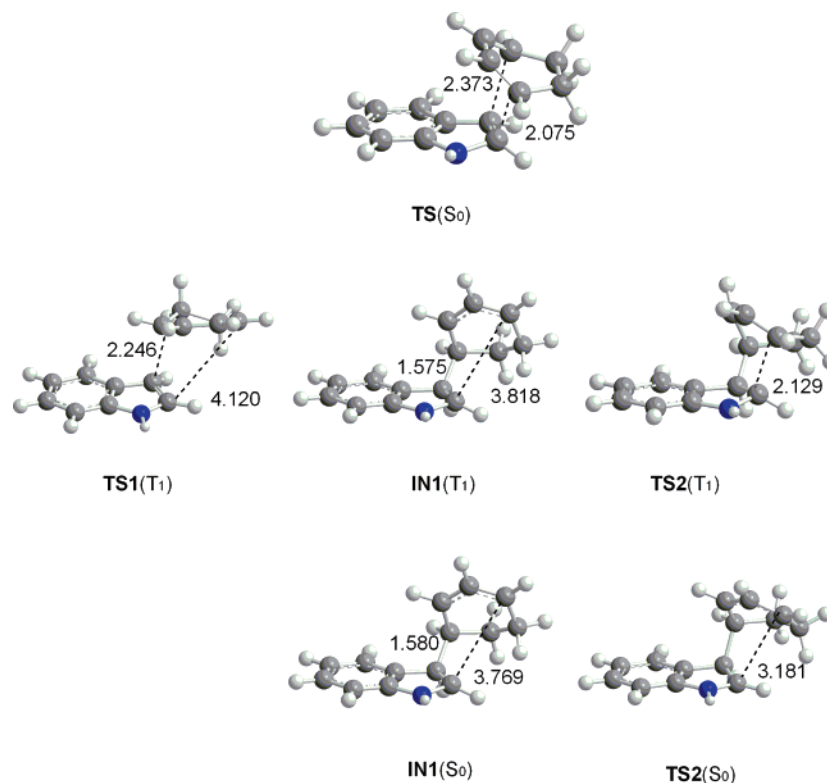


**FIGURE 3.** Geometries of the ground state ( $S_0$ ) and lowest triplet state ( $T_1$ ) transition structures and intermediates involved in the Diels–Alder reaction between InH and CHD. The bond lengths between the atoms directly involved in the reaction are given in angstroms.

**TABLE 2.** Total ( $E$ , in au) and Relative ( $\Delta E_{S_0}$ , Relative to the Ground  $S_0$  State, and  $\Delta E_{T_1}$ , Relative to the Lowest  $T_1$  State, in kcal mol $^{-1}$ ) Energies Involved in the Ground and Lowest Triplet Pathways Associated with Diels–Alder Reaction between InH and CHD and between the  $^3(\text{BT}\cdots\text{HIn})^*$  Exciplex and CHD

	$E$	$\Delta E_{S_0}$	$\Delta E_{T_1}$
InH( $S_0$ )	−363.816688		
CHD( $S_0$ ) <sup>a</sup>	−233.418936		
CHD( $T_1$ ) <sup>a</sup>	−233.339062		
BT-HIn( $T_1$ ) <sup>b</sup>	−1261.125197		
	InH( $S_0$ ) + CHD( $S_0$ )		
TS( $S_0$ )	−597.182264	33.5	
CA( $S_0$ )	−597.252613	−10.7	
	InH( $S_0$ ) + CHD( $T_1$ )		
TS1( $T_1$ )	−597.141443	59.1	9.0
IN1( $T_1$ )	−597.169984	41.2	−8.9
IN1( $S_0$ )	−597.169866	41.3	−8.9
TS2( $T_1$ )	−597.116806	74.6	24.4
TS2( $S_0$ )	−597.169727	41.4	−8.8
CA( $T_1$ )	−597.132272	64.9	14.7
	BT-HIn( $T_1$ ) + CHD( $S_0$ )		
TC( $T_1$ )	−1494.542091	59.0	1.3
TS3( $T_1$ )	−1494.542326	58.9	1.1
IN2( $T_1$ )	−1494.571383	40.7	−17.1
IN3( $T_1$ )	−1494.579886	35.3	−22.4
TS4( $T_1$ )	−1494.559233	48.3	−9.5
CA-BT( $T_1$ )	−1494.593104	27.0	−30.7
CA-BT( $S_0$ )	−1494.651695	−9.7	−67.5

<sup>a</sup> Reference 20. <sup>b</sup> Reference 18.

The extent of bond formation along a reaction pathway is provided by the concept of bond order (BO).<sup>21</sup> In TS( $S_0$ ) the BO values for the C3–C4 and C2–C7 bonds are 0.30 and 0.45,

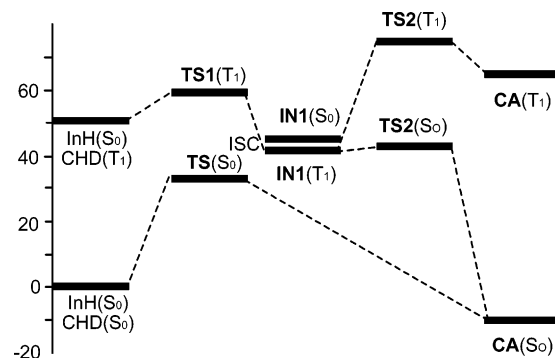


**FIGURE 4.** UB3LYP/6-31G\* energy profiles ( $\Delta E$ , in kcal mol $^{-1}$ ) for the ground ( $S_0$ ) and the triplet pathways associated with Diels–Alder cycloaddition between indole and 1,3-cyclohexadiene.

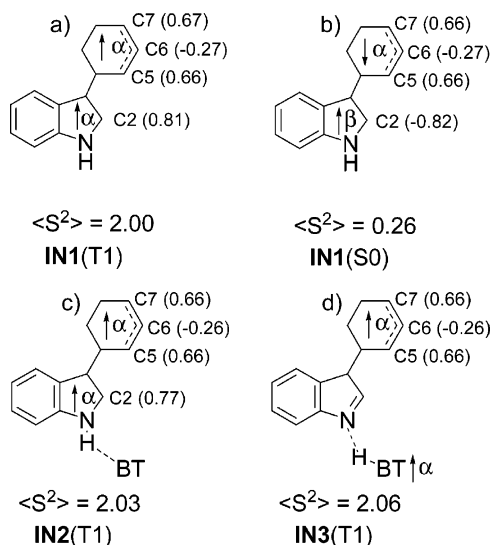
respectively. This is an asynchronous TS, as the C2–C7 is more advanced than C3–C4 bond formation. By contrast, in TS1( $T_1$ ) the BOs for C3–C4 and C2–C7 are 0.33 and 0.01, respectively. These BO values indicate that only the C3–C4 bond is being formed at this TS. For intermediates IN1( $T_1$ ) and IN1( $S_0$ ) the C3–C4 BO values are 0.94 and 0.93, respectively, indicating that this bond is already formed. However, the BOs between C2 and C7 remain at 0.00. In the transition states TS2( $T_1$ ) and TS2( $S_0$ ) the C2–C7 BO values are 0.38 and 0.10, respectively. Thus, TS2( $S_0$ ) is at a very early stage, in clear agreement with the very low barrier associated with ring closure and the exothermic character of the process.<sup>22</sup>

The electronic structures of TS1( $T_1$ ), IN1( $T_1$ ), and IN1( $S_0$ ) were investigated by the natural population analysis (NPA), and

(21) Wiberg, K. B. *Tetrahedron* **1968**, *24*, 1083.

(22) Hammond, G. S. *J. Am. Chem. Soc.* **1955**, *77*, 334.

**SCHEME 4.** Mulliken Atomic Spin Densities at the Biradical Intermediates **IN1(T<sub>1</sub>)**, **IN1(S<sub>0</sub>)**, **IN2(T<sub>1</sub>)**, and **IN3(T<sub>1</sub>)**.



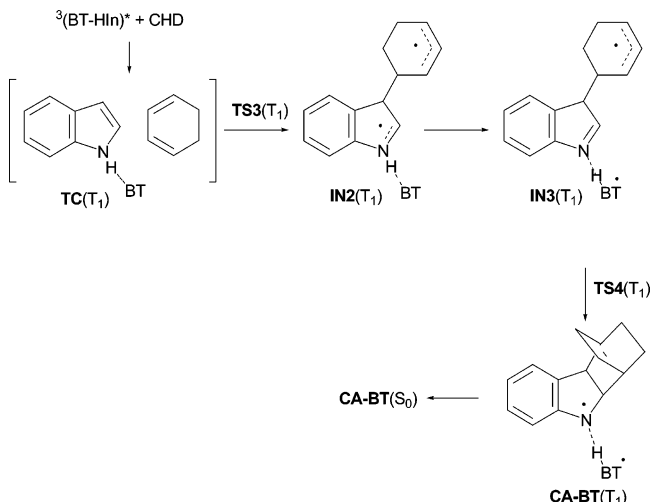
by the Mulliken atomic spin density analysis. The atomic charges in these species were partitioned between the InH and CHD frameworks. The net charge at InH is  $-0.05$  e in **TS1(T<sub>1</sub>)** and  $0.01$  e in **IN1(T<sub>1</sub>)** and **IN1(S<sub>0</sub>)**, indicating the nonpolar character of this cycloaddition. As expected, the atomic spin density in **TS1(T<sub>1</sub>)**, with a  $\langle S^2 \rangle$  value of 2.00, is mainly located at C2 (0.40) of the InH and at C5 (0.59), C6 ( $-0.48$ ), and C7 (0.70) of the CHD frameworks. In the case of intermediate **IN1(T<sub>1</sub>)**, with  $\langle S^2 \rangle$  value of 2.03, the atomic spin density is mainly located at C2 (0.81), C5 (0.66), C6 ( $-0.27$ ), and C7 (0.67). Initial  $\langle S^2 \rangle$  values for the singlet biradical stationary points, 1.03 (**IN1(S<sub>0</sub>)**) and 0.71 (**TS2(S<sub>0</sub>)**) become 0.26 (**IN1(S<sub>0</sub>)**) and 0.10 (**TS2(S<sub>0</sub>)**) after spin annihilation. These deviations of  $\langle S^2 \rangle$  from zero indicate that the biradical species are not pure singlet spin states.<sup>23</sup> A value of unity for  $\langle S^2 \rangle$  indicates a pure biradicaloid state, consisting of an equal mixture of singlet and triplet states.<sup>24</sup> At the intermediate **IN1(S<sub>0</sub>)** the atomic spin density is mainly located at C2 ( $-0.82$ ), C5 (0.66), C6 ( $-0.27$ ), and C7 (0.66). The analysis based on the atomic spin density indicates that the electronic structures of the intermediates are in agreement with biradical species where one  $\alpha$  (or  $\beta$ ) electron is mainly located at the C2 carbon atom of InH, while the second  $\alpha$  electron is delocalized over the allylic C5–C6–C7 framework belonging to the CHD residue. A schematic representation of these biradical species is given in Scheme 4 (a and b).

In summary, the photoinduced Diels–Alder reaction between InH and triplet CHD follows a two-step, two-state mechanism similar to that found for the photodimerization of CHD.<sup>20</sup> The reaction is initiated by attack of CHD(T<sub>1</sub>) to InH(S<sub>0</sub>), to give a biradical intermediate **IN1(T<sub>1</sub>)**. However, the large activation energy associated with ring closure at the T<sub>1</sub> excited-state precludes adiabatic cycloaddition. Instead, isc from **IN1(T<sub>1</sub>)** to **IN1(S<sub>0</sub>)** allows the subsequent ring closure to take place without any appreciable barrier. As the barrier associated with attack of CHD(T<sub>1</sub>) to InH(S<sub>0</sub>) is larger than that previously found for the attack of CHD(T<sub>1</sub>) to CHD(S<sub>0</sub>), formation of CHD dimers

(23) Goldstein, E.; Beno, B.; Houk K. N. *J. Am. Chem. Soc.* **1996**, *118*, 6036.

(24) Cramer, C. J.; Dulles, F. J.; Giesen, D. J.; Almlöf, J. *Chem. Phys. Lett.* **1995**, *245*, 165.

**SCHEME 5.** Diels–Alder Cycloaddition via a Triplet Ternary Complex



is expected to compete advantageously with Diels–Alder cycloaddition.

**Photoinduced Diels–Alder Reaction between InH and CHD in the Presence of BT.** For the photoinduced Diels–Alder reaction between CHD and the  $^3(\text{BT}\cdots\text{HIn})^*$  exciplex in the triplet state, UB3LYP/6-31G\* calculations support a stepwise mechanism. Here, a ternary complex, **TC(T<sub>1</sub>)** and **TS3(T<sub>1</sub>)** and **TS4(T<sub>1</sub>)**, two biradical intermediates, **IN2(T<sub>1</sub>)** and **IN3(T<sub>1</sub>)**, and the corresponding cycloadduct complex, **CA-BT(T<sub>1</sub>)**, were located and characterized (see Scheme 5). The geometries of all the stationary points are given in Figure 5, and the energetic results are summarized in Table 2.

Thus, **TC(T<sub>1</sub>)** is located only 1.3 kcal mol<sup>-1</sup> above the separated reactants: CHD and  $^3(\text{BT}\cdots\text{HIn})^*$ . For all the subsequent steps the reaction proceeds downhill (Figure 6). Thus, the energy barrier along this pathway is much lower than that associated with **TS1(T<sub>1</sub>)** or with the photochemical dimerization of CHD (activation enthalpy of 5 kcal mol<sup>-1</sup>).<sup>20</sup> This explains why the ratio CHD dimers/Diels–Alder cycloadducts is lower than expected from the relative rates determined for quenching of the triplet sensitizer by CHDs and InHs. Biradical intermediate **IN2(T<sub>1</sub>)** is located 17.1 kcal mol<sup>-1</sup> below the reactants. After a hydrogen (one proton and one electron) is transferred from the indole to the BT at **IN2(T<sub>1</sub>)**, a new intermediate, **IN3(T<sub>1</sub>)**, is formed. This intermediate is located 5.4 kcal mol<sup>-1</sup> below **IN2(T<sub>1</sub>)**. The ring-closure step at **IN3(T<sub>1</sub>)**, via **TS4(T<sub>1</sub>)**, presents a relatively low barrier (13.0 kcal mol<sup>-1</sup>) in contrast with the value of 33.4 kcal mol<sup>-1</sup> at **IN1(T<sub>1</sub>)**. Finally, adiabatic formation of the cycloadduct **CA-BT(T<sub>1</sub>)** is exothermic by  $-30.7$  kcal mol<sup>-1</sup>. Note that the adiabatic Diels–Alder reaction between InH(S<sub>0</sub>) and CHD(T<sub>1</sub>), to give **CA(T<sub>1</sub>)**, is endothermic by 14.7 kcal mol<sup>-1</sup>.

The geometries of **TS3(T<sub>1</sub>)**, **IN2(T<sub>1</sub>)**, **IN3(T<sub>1</sub>)**, and **TS4(T<sub>1</sub>)** are given in Figure 5. Note that at these TSs the BT framework presents different conformations as a consequence of the easy rotation of the N1–H and H–O bonds. The lengths of the C3–C4 and C2–C7 bonds being formed during the attack of CHD to the  $^3(\text{BT}\cdots\text{HIn})^*$  ternary complex are 2.246 and 4.094 Å at **TS3(T<sub>1</sub>)**. They are similar to those found for **TS2(T<sub>1</sub>)**, associated with the Diels–Alder reaction between InH(S<sub>0</sub>) and CHD(T<sub>1</sub>). The corresponding lengths for intermediates **IN2(T<sub>1</sub>)** (1.574, 3.884 Å) and **IN3(T<sub>1</sub>)** (1.569 and 3.744 Å) are closer to those

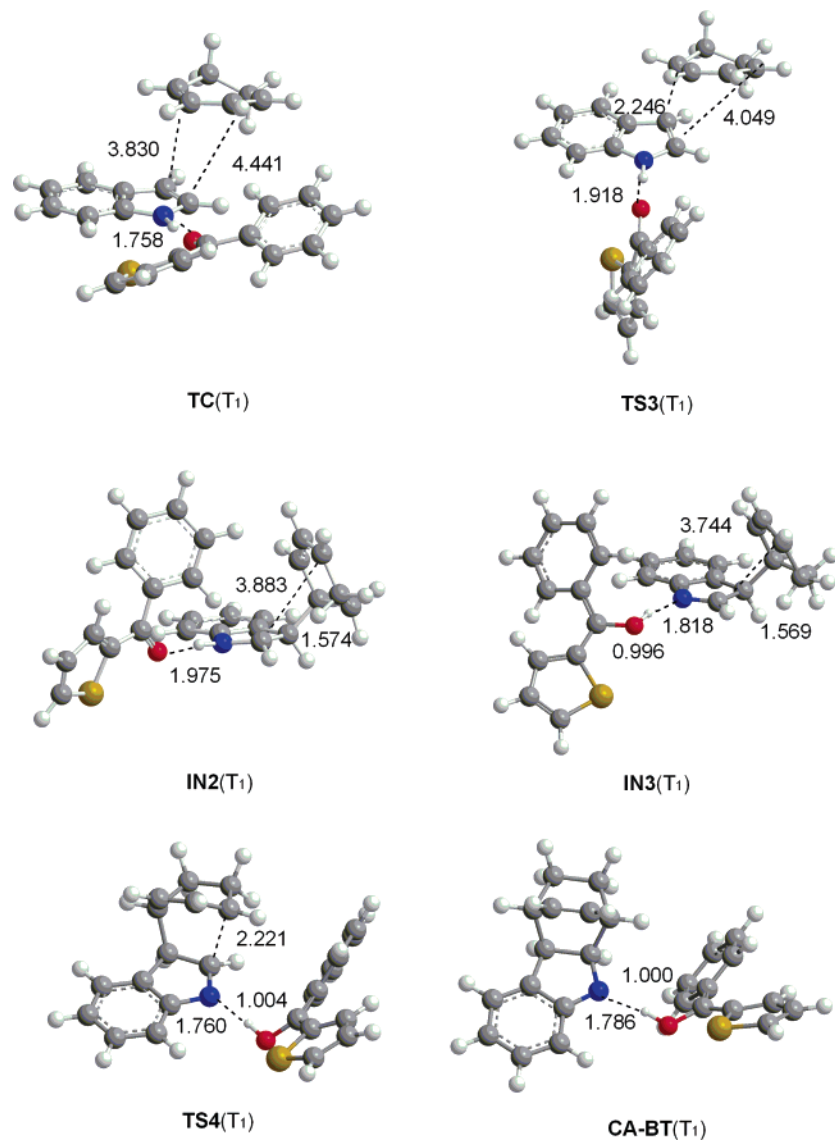


**FIGURE 5.** Geometries of the triplet state ( $T_1$ ) stationary points involved in the *endo* Diels–Alder reaction between the  $^3(\text{BT}\cdots\text{HIn})^*$  exciplex and CHD. The bond lengths between the atoms directly involved in the reaction are given in angstroms.

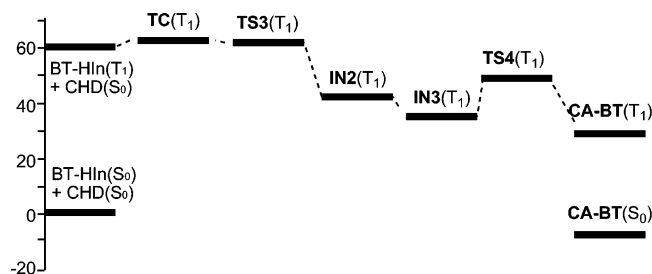


**FIGURE 6.** UB3LYP/6-31G\* Energy profiles ( $\Delta E$ , in kcal mol<sup>-1</sup>) for the triplet pathway associated with Diels–Alder cycloaddition between indole and 1,3-cyclohexadiene photosensitized by BT.

found for **IN1( $T_1$ )**, indicating that the C3–C4 bond is already formed. The N1–H and H–O lengths at these intermediates are 1.018 and 1.975 Å at **IN2( $T_1$ )** and 1.818 and 0.994 Å at **IN3( $T_1$ )**, respectively. These values show the hydrogen transfer from the indolic N–H to the BT carbonyl group at **IN2( $T_1$ )**. At **IN3( $T_1$ )**, these lengths are closer to those previously found for the BTH–In radical pair (1.797 and 0.997 Å).<sup>14</sup> Finally, at

**TS4( $T_1$ )** the lengths of the C2–C7 forming bond is 2.221 Å, while the N1–H and H–O lengths at this TS remain as 1.760 and 1.004 Å.

The BO values between the key carbon atoms involved in bond formation at **TS3( $T_1$ )**, associated with the attack of  $^3\text{CHD}$  to the  $(\text{BT}\cdots\text{HIn})$  exciplex, are 0.33 Å (C3–C4) and 0.01 Å (C2–C7). Therefore, only the C3–C4 bond is being formed at this TS. This process is completed in intermediate **IN2( $T_1$ )**, where the C3–C4 BO value is 1.00; at this stage, the BO value between C2 and C7 remains at 0.00. The N1–C2 BO values at **IN2( $T_1$ )** and **IN3( $T_1$ )** intermediates are 1.13 and 1.73, respectively. Finally, at **TS4( $T_1$ )**, associated with the ring closure, the C2–C7 BO value is 0.32.

The atomic charges at the stationary points along the reaction pathway are distributed between the BT, InH and CHD frameworks (see Table 3). In the ternary complex **TC( $T_1$ )** the situation is similar to that previously found for the  $^3(\text{BT}\cdots\text{HIn})^*$  exciplex, with a certain degree of charge transfer from the InH to the BT moiety.<sup>14</sup> However, in **TS3( $T_1$ )**, **IN2( $T_1$ )**, **IN3( $T_1$ )**, and **TS4( $T_1$ )** the net charges at the three frameworks are very



**TABLE 3.** Net Charges (in au) and Net Spin (in au) at the BT, InH, and CHD Fragments of Some Relevant Stationary Points Involved in Lowest Triplet State ( $T_1$ ) Pathways Associated with Diels–Alder Reaction between the  $^3(\text{BT}\cdots\text{HIn})^*$  Exciplex and CHD

	net charge			net spin		
	BT	InH	CHD	BT	InH	CHD
TC( $T_1$ )	−0.23	0.22	0.01	1.73	0.26	0.02
TS3( $T_1$ )	−0.04	0.08	−0.04	0.06	0.4	1.54
IN2( $T_1$ )	0.02	−0.03	0.01	0.01	0.98	1.02
IN3( $T_1$ )	−0.06	0.01	0.05	1.00	0.03	0.97
TS4( $T_1$ )	−0.07	−0.06	0.14	0.99	0.36	0.64
CA-BT( $T_1$ )	−0.07	0.02	0.05	0.99	0.96	0.05

small. Analysis of the atomic spin density provides a better understanding of this photoinduced Diels–Alder reaction. As in the  $^3(\text{BT}\cdots\text{HIn})^*$  exciplex, the two  $\alpha$  electrons of TC( $T_1$ ) associated with the lowest triplet state  $T_1$  are mainly located in the BT moiety. However, in TS3( $T_1$ ) the spin is mainly located at CHD. Both, net charge and spin distribution are similar to those found for TS1( $T_1$ ), associated with the attack of triplet CHD( $T_1$ ) to InH( $S_0$ ). The spin density at IN2( $T_1$ ) reveals the biradical nature of this species. As in the case of IN1( $T_1$ ), the spin density of IN2( $T_1$ ) is mainly located at C2 (0.77) and at C5 (0.66), C6 (−0.26) and C7 (0.66) (see c in Scheme 4). This analysis indicates that IN2( $T_1$ ) is a biradical intermediate with one  $\alpha$  electron mainly located at the InH framework and another one delocalized in the allylic framework of CHD. A different behavior is found at IN3( $T_1$ ). This biradical intermediate has one  $\alpha$  electron mainly delocalized in the allylic framework of CHD, and the other delocalized in the BTH framework (see d in Scheme 4). At TS4( $T_1$ ) the spin density at the BTH, In and CHD frameworks is 0.99, 0.36, and 0.64, respectively. These data indicate that TS4( $T_1$ ) is associated with the attack of the allyl radical to the imine in the IN3( $T_1$ ) intermediate. Finally, the atomic spin density at the CA-BT( $T_1$ ) cycloadduct is mainly located at the N atom of In (0.60), at the carbonyl carbon atom of BT (0.49) and at the two carbons belonging to the thienyl ring of BT (0.29 and 0.25).

**Role of BT in the Photocycloaddition between InH and CHD.** The present study allows to understand the role of BT in the photoinduced Diels–Alder reaction between InH and CHD. In the ternary complex TC( $T_1$ ), the atomic spin density analysis indicates a large biradical character. However, in TS3( $T_1$ ) the biradical is mainly located at the CHD framework. Therefore, energy transfer takes place along the reaction path between TC( $T_1$ ) and TS3( $T_1$ ), and attack of the nascent  $^3\text{CHD}$  to the indole in the TC( $T_1$ ) ternary complex takes place with a low barrier, leading to formation of a biradical intermediate IN2( $T_1$ ). Subsequent hydrogen transfer from N–H to the BT carbonyl group followed by ring closure gives rise to a ketyl-aminyl radical pair CA-BT( $T_1$ ), which mainly decays by back-hydrogen transfer, as previously found for the related BTH–In radical pairs.<sup>14</sup> Thus, ring closure of intermediate IN3( $T_1$ ) is energetically very favored, by contrast with the situation at IN1( $T_1$ ), where it is kinetically and thermodynamically disfavored as a consequence of formation of a very energetic CA( $T_1$ ). At IN3( $T_1$ ), the ring closure is associated with the attack of the allyl radical to the imine leading to CA-BT( $T_1$ ), which has the electron density delocalized in the BTH and in the indoline frameworks.

**Attempts to Detect the CA-BT( $T_1$ ) Radical Pair.** From the theoretical results, it was expected formation of CA-BT( $T_1$ ), basically an aminyl/BT ketyl radical pair. In an attempt to detect

this species, laser excitation (Nd:YAG, 10 ns laser pulse, 355 nm) of a deaerated dichloromethane solution containing **1a** (1.6 mM), **5b** (0.64 mM) and **6a** (0.32 mM) was performed. Transient absorption spectra were obtained with maxima at 340 and 390 nm, together with a broad absorption in the 350–650 nm region (see Figure S11A in Supporting Information), which decayed in the submicrosecond time scale.

Although the signal-to-noise ratio does not allow a conclusive assignment, this would be compatible with the added spectra of the BT ketyl radical (strong band at 350 nm and weak absorption between 540 and 600 nm)<sup>14</sup> and the expected N-centered radical derived from cycloadduct **8**. As a matter of fact, when a mixture of **8** and di-*tert*-butyl peroxide was photolyzed at 355 nm, to achieve H abstraction for the amino group, a transient absorption spectra were obtained with maximum in the 390–420 nm region and a featureless very noisy absorption extending until 650 nm (see Figure S11B in Supporting Information)

## Conclusions

The [4 + 2] cycloaddition of indoles with 1,3-cyclohexadienes can be photocatalyzed by triplet aromatic ketones. The experimental results agree with a pathway involving triplet ternary complexes. Theoretical DFT calculations strongly support this pathway where the  $^3(\text{BT}–\text{IH})^*$  triplet exciplex interacts with CHD and leads to a triplet cycloadduct-sensitizer complex, resulting from an adiabatic process occurring in the triplet energy surface. The ground-state product is formed after intersystem crossing.

## Experimental Section

**Standard Procedure for the Diels–Alder reactions.** To a deaerated dichloromethane (5 mL) solution of InH (0.02 M), CHD (0.04 M), and powdered NaHCO<sub>3</sub> (18 mg) was added acetyl chloride (0.02 M). Then, sensitizer (0.001 M) was added under nitrogen atmosphere. The irradiation was carried out in a photo-reactor equipped with eight UVA lamps ( $\lambda > 320$  nm,  $\lambda_{\text{max}}$  centered at 350 nm). The solutions were irradiated for 6–8 h, then filtered, washed with water, and dried over Na<sub>2</sub>SO<sub>4</sub>. The solvent was evaporated and the crude was analyzed by <sup>1</sup>H NMR. The products were isolated by column chromatography (polarity from hexane/ethyl acetate 7:1 to pure ethyl acetate) and further purified by HPLC).

**Computational Studies.** DFT calculations were carried out using the B3LYP<sup>25</sup> exchange-correlation functional, together with the standard 6-31G\* basis set.<sup>26</sup> For all calculations the unrestricted formalism (UBLYP) was employed. Recent studies devoted to reaction involving biradical intermediates have shown that the energetic results obtained at the UB3LYP/6-31G\* level are in reasonable agreement with those obtained by single-point energy calculations at the very computing demanding CCSD(T)/6-31G\*<sup>20,27</sup> and CCSD(T)/cc-pVDZ<sup>28</sup> level. Optimizations were carried out using the Berny analytical gradient optimization method.<sup>29</sup>

(25) (a) Becke, A. D. *J. Chem. Phys.* **1993**, *98*, 5648–5652. (b) Lee, C.; Yang, W.; Parr, R. G. *Phys. Rev. B* **1988**, *37*, 785.

(26) Hehre, W. J.; Radom, L.; Schleyer, P. v. R.; Pople, J. A. *Ab initio Molecular Orbital Theory*; Wiley: New York, 1986.

(27) Isobe, H.; Takano, Y.; Kitagawa, Y.; Kawakami, T.; Yamanaka, S.; Yamaguchi, K.; Houk, K. N. *J. Phys. Chem. A* **2003**, *107*, 682–694.

(28) Schreiner, P. R.; Navarro-Vázquez, A.; Prall, M. *Acc. Chem. Res.* **2005**, *38*, 29.

(29) (a) Schlegel, H. B. *J. Comput. Chem.* **1982**, *3*, 214–218. (b) Schlegel, H. B. *Geometry Optimization on Potential Energy Surface. In Modern Electronic Structure Theory*; Yarkony, D. R., Ed.; World Scientific Publishing: Singapore, 1994.

The stationary points were characterized by frequency calculations, to verify that the transition structures (TSs) have one and only one imaginary frequency. The intrinsic reaction coordinate (IRC)<sup>30</sup> path was traced in order to check the energy profiles connecting each TS with the two associated minima of the proposed mechanism by using the second-order González-Schlegel integration method.<sup>31</sup> The electronic structures of stationary points were analyzed by the natural bond orbital (NBO) method.<sup>32</sup> Natural charges were obtained by the natural population analysis (NPA).<sup>33</sup> All calculations were carried out with the Gaussian 03 suite of programs.<sup>34</sup>

**Laser Flash Photolysis.** Laser flash photolysis experiments were carried out by using the third harmonics (355 nm) of a pulsed Nd:YAG laser. The pulse duration was 10 ns, and the energy of the laser beam was 18 mJ/pulse. A xenon lamp was employed as detecting light source. The laser apparatus consisted of the pulsed laser, the Xe lamp, a monochromator, a photomultiplier (PMT) system, and an oscilloscope. The output signal was transferred to a personal computer for data analysis.

**Acknowledgment.** We thank the Ministerio de Educación y Ciencia (Project BQU2002-00377, CTQ2004-03811, doctoral

fellowship to M.G.B., and RyC contract to S.-E.S.) and the Universidad de Valencia (Project UV-AE-06-3) for generous support of this work.

**Supporting Information Available:** Synthesis of cycloadduct **8** and spectroscopic data for compounds **7b**, **7d** and **8**, as well as additional transient absorption spectra and Stern–Volmer plots for BT and BP quenching by **5b**. Cartesian coordinates of the ground and lowest triplet state transition structures and intermediates involved in the Diels–Alder reaction between InH and CHD and between the <sup>3</sup>(BT•••HIn)\* exciplex and CHD. This material is available free of charge via the Internet at <http://pubs.acs.org>.

JO061078M

(34) Frisch, M. J.; Trucks, G. W.; Schlegel, H. B.; Scuseria, G. E.; Robb, M. A.; Cheeseman, J. R.; Montgomery, J. A., Jr.; Vreven, T.; Kudin, K. N.; Burant, J. C.; Millam, J. M.; Iyengar, S. S.; Tomasi, J.; Barone, V.; Mennucci, B.; Cossi, M.; Scalmani, G.; Rega, N.; Petersson, G. A.; Nakatsuji, H.; Hada, M.; Ehara, M.; Toyota, K.; Fukuda, R.; Hasegawa, J.; Ishida, M.; Nakajima, T.; Honda, Y.; Kitao, O.; Nakai, H.; Klene, M.; Li, X.; Knox, J. E.; Hratchian, H. P.; Cross, J. B.; Bakken, V.; Adamo, C.; Jaramillo, J.; Gomperts, R.; Stratmann, R. E.; Yazyev, O.; Austin, A. J.; Cammi, R.; Pomelli, C.; Ochterski, J. W.; Ayala, P. Y.; Morokuma, K.; Voth, G. A.; Salvador, P.; Dannenberg, J. J.; Zakrzewski, V. G.; Dapprich, S.; Daniels, A. D.; Strain, M. C.; Farkas, O.; Malick, D. K.; Rabuck, A. D.; Raghavachari, K.; Foresman, J. B.; Ortiz, J. V.; Cui, Q.; Baboul, A. G.; Clifford, S.; Cioslowski, J.; Stefanov, B. B.; Liu, G.; Liashenko, A.; Piskorz, P.; Komaromi, I.; Martin, R. L.; Fox, D. J.; Keith, T.; Al-Laham, M. A.; Peng, C. Y.; Nanayakkara, A.; Challacombe, M.; Gill, P. M. W.; Johnson, B.; Chen, W.; Wong, M. W.; Gonzalez, C.; Pople, J. A. *Gaussian 03*, Revision C.02; Gaussian, Inc.: Wallingford CT, 2004.

(30) Fukui, K. *J. Phys. Chem.* **1970**, *74*, 4161–4163.

(31) (a) González, C.; Schlegel, H. B. *J. Phys. Chem.* **1990**, *94*, 5523.

(b) González, C.; Schlegel, H. B. *J. Chem. Phys.* **1991**, *95*, 5853–5860.

(32) (a) Reed, A. E.; Weinhold, F. *J. Chem. Phys.* **1983**, *78*, 4066. (b)

Reed, A. E.; Curtiss, L. A.; Weinhold, F. *Chem. Rev.* **1988**, *88*, 899–926.

(33) Reed, A. E.; Weinstock, R. B.; Weinhold, F. *J. Chem. Phys.* **1985**, *83*, 735.